

The second order nonlinear conductance of a two-dimensional mesoscopic conductor

Wei-Dong Sheng^{1,*}, Jian Wang¹, and Hong Guo²

¹ *Department of Physics,
The University of Hong Kong,
Pokfulam Road, Hong Kong.*

² *Centre for the Physics of Materials,
Department of Physics, McGill University,
Montreal, Quebec, Canada H3A 2T8.*

We have investigated the weakly non-linear quantum transport properties of a two-dimensional quantum conductor. We have developed a numerical scheme which is very general for this purpose. The nonlinear conductance is computed by explicitly evaluating the various partial density of states, the sensitivity and the characteristic potential. Interesting spatial structure of these quantities are revealed. We present detailed results concerning the crossover behavior of the second order nonlinear conductance when the conductor changes from geometrically symmetrical to asymmetrical. Other issues of interests such as the gauge invariance are also discussed.

PACS number: 73.20.Dx, 73.49.Ei, 73.40.Gk, 73.50.Fq

1 Introduction

Nonlinear phenomena in electric conduction play the most important role in many electronic applications ranging from single units such as a diode or a transistor to entire circuits. For extremely small systems with mesoscopic or atomic length scales, such as those which can now be routinely fabricated using nano-technology, quantum transport dominates conduction. While we now have a very good understanding of linear quantum transport phenomena in nano-systems where quantum coherence plays a vital role, the nonlinear quantum transport properties of mesoscopic conductors have received relatively less attention. In this regard, several important research results have been reported in recent years[1, 2, 3, 4, 5]. Experimentally, Taboryski *et. al.*[5] have reported observations of nonlinear and asymmetric conductance oscillations in quantum point contacts at small bias voltages. They found that the non-Ohmic and asymmetric behavior causes a rectified DC signal as the response to an applied AC current. On the theoretical side several directions have been explored. Wingreen *et. al.*[3] have presented a general formulation to deal with the situation of a non-linear and time-dependent current going through a small interacting region where electron energies can be changed by time-dependent voltages. De Vegvar[4] has studied the low frequency second-harmonic transport response of multiprobe mesoscopic conductors using a perturbation theory in the framework of Kubo formula and found that the low frequency second-harmonic current is a non-Fermi-surface quantity. At the same time, Büttiker and his co-workers[6, 1, 7] have advanced a current conserving theory for the frequency dependent transport. This theory can be applied to discuss the non-linear behavior of mesoscopic samples. It has been recognized[8] that in non-linear coherent quantum transport, it is essential to consider the internal self-consistent potential in order to have the theory satisfy the gauge invariance condition. This is a fundamental condition which requires that all physical properties predicted by a theory can not change if there is a global voltage shift. Recently, Christen and Büttiker[8] have investigated the rectification coefficient of a quantum point contact and the non-linear current-voltage characteristic of a resonant level in a double barrier structure using this theory of gauge invariant non-linear conductance.

Clearly it is important and useful to further investigate nonlinear quantum transport phenomena in coherent quantum conductors. In particular, detailed predictions of nonlinear conductance of two-dimensional (2D) systems warrant to be made because these systems can now be fabricated in many laboratories.

Unfortunately due to various technical difficulties, especially the difficulty of evaluating a quantity called *sensitivity* (see below), so far the application of Büttiker's theory[8] has largely been limited to quasi-1D systems. For 2D conductors, in general some numerical calculation is needed and this has recently been carried out by two of the authors[9] to study the admittance of a T-shaped conductor which is related to the *linear* order transmission function. The nonlinear conductance for a 2D conductor, on the other hand, has been investigated for a very special and exactly solvable model which is a quasi-1D ballistic wire with a δ -function impurity confined inside[10, 11]. Since it is exactly solvable[10], the sensitivity can be computed in a closed form thereby overcoming the technical difficulties associated with the theoretical formalism. To the best of our knowledge, this was the only explicit computation of the weakly nonlinear conductance from the gauge invariant AC transport theory for a 2D system where mode mixing is the most important characteristic. However we note that in order to apply the theoretical formalism to a wide range of 2D mesoscopic conductors, a more general numerical method must be developed and various physical issues cleared. The purpose of this article is to report our development of such a numerical method, and to investigate the weakly nonlinear transport properties of a truly 2D conductor.

As we have noted from the previous investigation of the exactly solvable model[10], for a geometrically symmetric system the second order non-linear conductance G_{111} must be zero from a general argument (see below). Hence the non-linear effect, *i.e.* a non-zero $G_{\alpha\beta\gamma}$, obtained in Ref. [10] is a delicate effect of the asymmetric scattering boundary[12]. Such an asymmetry is brought about when the δ -function scatterer is not located at the center of the scattering volume[10]. Already, very interesting and physically revealing behavior of the local current response (the sensitivity) has been found. In this work, on the other hand, we shall focus on a much more general situation by investigating the 2D conductor depicted in Fig. (1) where the scattering volume is defined by the shaded area. The two leads with width W are assumed to extend far away from the scattering volume. The shape of the side stub is controlled by the parameter H as shown in Fig. (1), hence various different 2D systems can be generated by varying H . For $H = W$, the scattering volume is a geometrically asymmetric system, but the asymmetry is only due to the *asymmetric* locations of the scattering volume boundary. For this case we thus expect that the physics should be similar to those obtained in Ref. [10]. For $H = 2W$, the scattering volume becomes a geometrically symmetric system where $G_{\alpha\beta\gamma}$ must be zero. For other values of H between W and $2W$, the scattering volume is intrinsically asymmetric. By

varying H , we shall study the crossover behavior of G_{111} between the symmetric and asymmetric situations.

Our results show that the external (the internal) response of the second order non-linear conductance changes sign from negative (positive) to positive (negative) near a quantum resonant point. The cancellation of the external and internal responses results in a much smaller second order non-linear conductance G_{111} , *i.e.*, G_{111} is one order of magnitude smaller than the external or internal response. The behavior of G_{111} is non-monotonic when changing the parameter H in the range $W \leq H \leq 2W$: this is because G_{111} is very small at $H = W$ as it is solely due to the asymmetric scattering boundary, it increases as H is increased, and it is zero at $H = 2W$. Another result of our analysis concerns the gauge invariant condition $\sum_{\gamma} G_{\alpha\beta\gamma} = 0$. It turns out that for systems with a finite scattering volume as those of any numerical calculations, if the global partial density of states (GPDOS) is computed from the *energy* derivatives of the scattering matrix, it was found[10] that a correction term must be added to satisfy the gauge invariant condition. For the exactly solvable model studied in our previous work[10], this correction term has been derived[10] analytically. We shall examine this effect for the conductor studied here.

The paper is organized as follows. In the next section we shall briefly review the gauge invariant theory for non-linear transport developed by Büttiker[1]. The method of calculating various quantities needed for non-linear conductance and our results are presented in sections 3 and 4. The last section serves as a brief summary.

2 The formalism

The gauge invariant formalism of nonlinear transport has been developed and clearly discussed in Ref. [8] and we refer interested reader to the original work. In this section, we shall outline the main steps of the application of this formalism for our calculation. For a multi-probe mesoscopic conductor, the current through probe α is given by[1, 8]

$$I_{\alpha} = \frac{2e}{h} \sum_{\beta} \int dE f(E - E_F - eV_{\beta}) A_{\alpha\beta}(E, \{V_{\gamma}\}), \quad (1)$$

where $f(E)$ is the Fermi distribution function, and

$$A_{\alpha\beta}(E, \{V_{\gamma}\}) = Tr[\mathbf{1}_{\alpha} \delta_{\alpha\beta} - \mathbf{s}_{\alpha\beta}^{\dagger}(E, \{V_{\gamma}\}) \mathbf{s}_{\alpha\beta}(E, \{V_{\gamma}\})] \quad (2)$$

are the screened (negative) transmission functions which are expressed in terms of the scattering matrix $\mathbf{s}_{\alpha\beta}$. For weakly non-linear transport, Eq.(1) can be expanded with respect to the voltages V_β . For a conductor which has only two probes, up to the second order nonlinear term such an expansion leads to the following equation[8, 10],

$$I_1 = G_{11}(V_1 - V_2) + G_{111}(V_1 - V_2)^2 \quad , \quad (3)$$

where G_{11} is the usual linear conductance and G_{111} is the second order nonlinear conductance which we wish to compute for the conductor of Fig. (1).

It can further be proven[8] that $G_{\alpha\beta\gamma}$ is the sum of two terms which are the external and internal contributions:

$$G_{\alpha\beta\gamma} = G_{\alpha\beta\gamma}^e + G_{\alpha\beta\gamma}^i \quad (4)$$

where the external contribution can be obtained using the free electron scattering theory by evaluating the energy derivatives of the scattering matrix,

$$G_{\alpha\beta\gamma}^e = \frac{e^2}{h} \int dE (-\partial_E f) e \partial_E A_{\alpha\beta} \delta_{\beta\gamma} \quad . \quad (5)$$

The internal contribution, on the other hand, is much more difficult to obtain because it depends on the potential derivatives of the scattering matrix,

$$G_{\alpha\beta\gamma}^i = \frac{e^2}{h} \int dE (-\partial_E f) (\partial_{V_\gamma} A_{\alpha\beta} + \partial_{V_\beta} A_{\alpha\gamma}) \quad . \quad (6)$$

The reason why this is difficult to evaluate is because when the voltage of a probe V_γ changes, the entire potential landscape of the scattering volume will change accordingly through the electron-electron interactions. Hence the internal contribution to the nonlinear conductance can be obtained only after an interacting electron problem has been solved[8]. This is a very difficult task and so far has not been successfully implemented in a numerical scheme. However if we can use the Thomas-Fermi linear screening model, which is more appropriate for metallic conductors, the internal contribution can be computed through the evaluation of quantities called sensitivity and characteristic potential[8]. It can be shown[8] that the potential derivative of the transmission function is given as,

$$\partial_{V_\gamma} A_{\alpha\beta} = 4\pi \int d^3\mathbf{r} \eta_{\alpha\beta}(\mathbf{r}) u_\gamma(\mathbf{r}) \quad (7)$$

where

$$\eta_{\alpha\beta}(\mathbf{r}) = \frac{1}{4\pi} \frac{\delta A_{\alpha\beta}}{\delta U(\mathbf{r})} = -\frac{1}{4\pi} Tr(\mathbf{s}_{\alpha\beta}^\dagger \frac{\delta \mathbf{s}_{\alpha\beta}}{\delta U(\mathbf{r})} + \mathbf{s}_{\alpha\beta} \frac{\delta \mathbf{s}_{\alpha\beta}^\dagger}{\delta U(\mathbf{r})}) \quad (8)$$

is called *sensitivity*[13] which measures the local electric current response to an external perturbation. $u_\gamma(\mathbf{r})$ is the characteristic potential which measures the variation of the potential landscape of the scattering volume due to the perturbation[1]. Within the Thomas-Fermi screening model, it is given by

$$u_\gamma(\mathbf{r}) = \frac{dn(\mathbf{r}, \gamma)}{dE} / \frac{dn(\mathbf{r})}{dE} . \quad (9)$$

Here the local partial density of states (LPDOS) $dn(\mathbf{r}, \gamma)/dE$ is called the injectivity and is given by[14] the scattering wavefunctions,

$$\frac{dn(\mathbf{r}, \gamma)}{dE} = \sum_n \frac{|\Psi_{\gamma n}(\mathbf{r})|^2}{hv_{\gamma n}} , \quad (10)$$

where $v_{\gamma n}$ is the electron velocity for the propagating channel labeled by n , and $dn(\mathbf{r})/dE = \sum_\alpha dn(\mathbf{r}, \alpha)/dE$ is the total local density of states.

From the weakly nonlinear conductance formalism summarized above, several observations are in order. First, from an application of this formalism point of view, a crucial step is the evaluation of the sensitivity $\eta_{\alpha\beta}$ which depends on the functional derivative of the scattering matrix with respect to the local potential variation. The latter is caused by the external perturbation, *i.e.* the change of the electrochemical potential at a lead. We are aware of two ways of calculating the sensitivity[13]. The first is to evaluate $\delta\mathbf{s}_{\alpha\beta}/\delta U$ directly by introducing a δ -function of infinitesimal strength δU inside the scattering region. Alternatively, one can calculate it using the retarded Green's function. For a 2D system, in general the Green's function can not be obtained explicitly except in very special cases such as that studied in Ref. [11], hence we shall use the first method by directly computing the sensitivity. As a second observation which is physically important[12], we can discuss the general behavior of the nonlinear conductance G_{111} . From Eq. (3), for a symmetric scattering volume with scattering potential $U(x, y) = U(-x, y)$ where x is the propagation direction, we must have $-I_1$ if V_1 and V_2 are interchanged. Hence we conclude that for a symmetric scattering volume there is no quadratic terms, *i.e.*, $G_{111} = 0$. On the other hand, in general $G_{111} \neq 0$ for geometrically asymmetrical systems. Finally, due to the current conservation and the gauge invariance condition, namely the entire physics is independent of a global voltage shift, it is not difficult to prove[1, 8, 14]

$$\sum_\alpha G_{\alpha\beta\gamma} = \sum_\beta G_{\alpha\beta\gamma} = \sum_\gamma G_{\alpha\beta\gamma} = 0 . \quad (11)$$

Our results will allow a direct confirmation of this equation.

3 Numerical method

There are several ways to solve the scattering matrix of 2D ballistic conductors, such as the mode-matching method[15], the recursive Green's function method[16, 17, 18], and the finite-element method[19, 20]. However we found that all these methods are not particularly easy to apply here because we need not only the scattering matrix, but also the sensitivity $\eta_{\alpha\beta}$. For this purpose, we found that a technique for computing scattering matrix which is developed in Ref. [21] is quite useful and we shall discuss, in some detail, our numerical procedure for finding $\eta_{\alpha\beta}$.

In particular, we construct a global scattering matrix using the mode-matching method of Ref. [21]. For a scattering volume which is not uniform along its longitudinal direction, we divide it into a number of uniform sections, *e.g.*, the asymmetric cavity as shown in Fig. (1) can be divided into four uniform sections. The scattering matrix associated with the n -th section \mathbf{S}_n is the composition of two individual scattering matrices \mathbf{S}_n^f and \mathbf{S}_n^i , *i.e.*, $\mathbf{S}_n = \mathbf{S}_n^f \otimes \mathbf{S}_n^i$ where \otimes is the operator which denotes the composition of two scattering matrices[22]. Here \mathbf{S}_n^f describes the free propagation from the left end of the n -th section to its right end and is given by

$$\mathbf{S}_n^f(L_n) = \begin{bmatrix} \mathbf{0} & \mathbf{P}_n \\ \mathbf{P}_n & \mathbf{0} \end{bmatrix} \quad (12)$$

where \mathbf{P}_n is a diagonal matrix with elements $(\mathbf{P}_n)_{mm} = e^{ik_n^m L_n}$, k_n^m is the longitudinal wave number for the m -th mode and L_n is the length of the n -th section. The scattering process at the interface between two adjacent sections (the n -th and $(n+1)$ -th sections) is described by \mathbf{S}_n^i . Care must be taken when matching the wavefunctions of two sections with different widths at the section boundary. If the width of the n -th section W_n is not greater than W_{n+1} , we have

$$\mathbf{S}_n^i = \begin{bmatrix} -\mathbf{C}^T & \mathbf{I} \\ \mathbf{K}_n & \mathbf{C}\mathbf{K}_{n+1} \end{bmatrix}^{-1} \begin{bmatrix} \mathbf{C}^T & -\mathbf{I} \\ \mathbf{K}_n & \mathbf{C}\mathbf{K}_{n+1} \end{bmatrix} \quad (13)$$

where \mathbf{K}_n is a diagonal matrix with diagonal element k_n^m , and \mathbf{I} is a unit matrix. \mathbf{C} is a matrix which denotes the coupling between the transverse modes in the two sections and its elements are given by $C_{ij} = \langle \phi_n^i | \phi_{n+1}^j \rangle$ where ϕ_n^i is the i th transverse mode in the n th section. \mathbf{C}^T is the transpose of the matrix \mathbf{C} . On the other hand if $W_n > W_{n+1}$, we have

$$\mathbf{S}_n^i = \begin{bmatrix} -\mathbf{I} & \mathbf{C} \\ \mathbf{C}^T \mathbf{K}_n & \mathbf{K}_{n+1} \end{bmatrix}^{-1} \begin{bmatrix} \mathbf{I} & -\mathbf{C} \\ \mathbf{C}^T \mathbf{K}_n & \mathbf{K}_{n+1} \end{bmatrix} \quad (14)$$

Once the scattering matrix for each section is known, the global scattering matrix can be easily constructed by the composition of all the individual scattering matrices,

$$\mathbf{S} = \mathbf{S}_1 \otimes \mathbf{S}_2 \otimes \dots \otimes \mathbf{S}_{M-1} \quad (15)$$

where M is the total number of sections.

It should be noted that the global scattering matrix \mathbf{S} calculated this way is different from the standard one[17] which only connects the outgoing wave to the incoming wave. Here, the global scattering matrix \mathbf{S} involves the non-propagating channels as well and does not satisfy the unitarity condition. In order to obtain a physical scattering matrix which we denote by the lower case \mathbf{s} , we first rewrite global \mathbf{S} in the form of 2×2 subblocks and obtain four sub-matrices \mathbf{S}_{ij} where $(i, j = 1, 2)$. Then for each sub-matrix \mathbf{S}_{ij} we build a new matrix \mathbf{s}_{ij} constructed by the first N_0 rows and columns of \mathbf{S}_{ij} , where N_0 is the number of propagating channels. By writing the four newly constructed matrices in the form of 2×2 blocks, a $2N_0$ -dimensional scattering matrix \mathbf{s} is obtained which is the true scattering matrix that connects the outgoing wave to the incoming wave. In order to obtain a unitary scattering matrix \mathbf{s} , one should further take a unitary transformation.

$$\begin{aligned} \mathbf{s} &= \mathbf{A} \mathbf{s} \mathbf{A}^{-1} \\ \mathbf{A} &= \begin{bmatrix} \mathbf{V} & \mathbf{0} \\ \mathbf{0} & \mathbf{V} \end{bmatrix} \end{aligned} \quad (16)$$

where \mathbf{V} is a N_0 -dimensional diagonal matrix with diagonal element $\sqrt{k_n}$.

The above procedures can easily be modified to compute the sensitivity $\eta_{\alpha\beta}(\mathbf{r})$. For this purpose, we shall make use of a δ -function impurity to calculate the functional derivatives of the scattering matrices $\delta\mathbf{s}_{\alpha\beta}/\delta U(\mathbf{r})$. This is achieved as follows. We put a δ -function impurity with infinitesimal strength γ , $V(\mathbf{r}) = \gamma\delta(\mathbf{r} - \mathbf{r}_0)$, at arbitrary positions $\mathbf{r} = \mathbf{r}_0$ in the scattering volume. We then calculate the scattering matrix $\mathbf{s}_{\alpha\beta}$ as a function of γ . Finally we use a five-point numerical derivative to evaluate $\delta\mathbf{s}_{\alpha\beta}/\delta U(\mathbf{r}) \equiv \partial\mathbf{s}_{\alpha\beta}/\partial\gamma|_{\gamma=0}$. With this result we can obtain the sensitivity from Eq. (8).

The scattering matrix can still be obtained using the approach discussed above even including the δ -function impurity. In fact it has been derived in the presence of a magnetic field by Tamura and Ando[22]. Here we give the expression in the absence of the field[23]. Suppose the δ -function impurity is located in the n -th section at position $\mathbf{r}_0 = (x_0, y_0)$, where x_0 and y_0 is the distance from the left and bottom boundary of the section respectively. The scattering matrix associated

with this section is then given by

$$\mathbf{S}_n = \mathbf{S}_n^f(x_0) \otimes \mathbf{S}_n^\delta \otimes \mathbf{S}_n^f(L_n - x_0) \otimes \mathbf{S}_n^i \quad . \quad (17)$$

Here \mathbf{S}_n^δ describes the scattering process associated with the δ -function impurity and is given by[23]

$$\mathbf{S}_n^\delta = \begin{bmatrix} -\mathbf{I} & \mathbf{I} \\ i\mathbf{K}_n - \mathbf{\Gamma} & i\mathbf{K}_n \end{bmatrix}^{-1} \begin{bmatrix} \mathbf{I} & -\mathbf{I} \\ i\mathbf{K}_n + \mathbf{\Gamma} & i\mathbf{K}_n \end{bmatrix} \quad (18)$$

where the matrix $\mathbf{\Gamma}$ describes the mode-mixing effect due to the δ -function impurity and its matrix elements are given by $\Gamma_{pq} = 2\gamma \sin(p\pi y_0/W_n) \sin(q\pi y_0/W_n)/W_n$ with W_n being the width of the section. With the δ -function included this way, we can again apply our method, Eq. (15), to compute the scattering matrix $\mathbf{s} = \mathbf{s}(\gamma)$ and complete the numerical derivatives discussed in the last paragraph.

To end this section, we briefly mention two other points. First, the characteristic potential as given by Eq. (9) is evaluated using the scattering wavefunction which can be calculated in two ways, directly or indirectly. One can directly compute the wavefunction using the mode matching method[15] or finite element method[19, 20]. Or one can compute the wavefunction ($|\Psi|^2$) indirectly by computing the local partial DOS called emissivity defined as[14]

$$\frac{dn(\alpha, \mathbf{r})}{dE} = -\frac{1}{4\pi i} \sum_{\beta} Tr(\mathbf{s}_{\alpha\beta}^\dagger \frac{\delta \mathbf{s}_{\alpha\beta}}{\delta eU(\mathbf{r})} - \mathbf{s}_{\alpha\beta} \frac{\delta \mathbf{s}_{\alpha\beta}^\dagger}{\delta eU(\mathbf{r})}) \quad (19)$$

The microreversibility of the scattering matrix implies,

$$\frac{dn(\alpha, \mathbf{r}, B)}{dE} = \frac{dn(\mathbf{r}, \alpha, -B)}{dE} \quad (20)$$

where B is the magnetic field. We will use Eqs.(10),(19), and (20) to compute the wavefunction $|\Psi|^2$ since we have to compute the scattering matrix or $\delta \mathbf{s}/\delta U(\mathbf{r})$ anyway for the sensitivity. Second, the energy derivatives of the transmission function, which determines the external response contribution to the second order nonlinear conductance, is evaluated using a five point numerical difference. These procedures are the same as that of our earlier work[9].

4 Results

As a first result we plot in Fig. (2) the sensitivity $\eta_{11}(\mathbf{r})$ at three different positions inside the scattering volume, $\mathbf{r}_1 = (0.5W, 0.5W)$, $\mathbf{r}_2 = (0.5W, 1.25W)$,

and $\mathbf{r}_3 = (1.25W, 0.625W)$, as a function of the normalized electron momentum $k_F W/\pi$ where k_F is the electron Fermi wave number. These results are for an asymmetric system (see Fig. (1)) with the parameter $H = 1.25W$. As discussed in Section 2 $\eta_{\alpha\beta}$ appears naturally in the theoretical formalism, and it essentially describes the local (internal) electric current response of the scattering problem when there is a small local potential change. It is related to the real part of the diagonal elements of the scattering Green's function[13]. From Fig. (2), we see that different positions inside the scattering volume have quite different internal responses in terms of the peak heights of the apparent resonance behavior. On the other hand, the peak positions occur at the same electron energies given by $k_F W/\pi$ for η_{11} at all three positions. We have checked (see below and Fig. (5b)) that the peak positions also coincide with those of the conductance. Hence we may conclude that the local current response can have sharp changes, from positive values to negative values, across the energy of a resonance which also mediates a resonance transmission. For the two positions \mathbf{r}_1 and \mathbf{r}_2 which are located in the left part of the cavity, the shapes of the sensitivities are more similar to each other. This is to be compared with that of the position \mathbf{r}_3 which is located in the right part of the cavity. The differences are evident from the three curves of Fig. (2).

To get a more intuitive picture of the spatial dependence of the sensitivity, in Fig. (3) we plot $\eta_{11}(\mathbf{r})$ in the entire scattering volume for two different values of the electron momentum ($H = 1.25W$). First is for $k_F W/\pi = 1.715$ which is off resonance, while the second is for $k_F W/\pi = 1.795$ which is on resonance. From the lower panel of Fig. (3) which corresponds to the resonant energy, the behavior of η_{11} is reminiscent of a standing wave which is in accordance to our usual picture of a quantum resonance. The positions \mathbf{r}_1 and \mathbf{r}_2 of Fig. (2) are located at a peak of the sensitivity profile while \mathbf{r}_3 is at a valley. This explains why in Fig. (2) we observe the large resonant peak at \mathbf{r}_1 and \mathbf{r}_2 but not at \mathbf{r}_3 . When off resonance, the upper panel of Fig. (3) shows less regular patterns for η_{11} . Hence the local current response can behave regularly or less regularly depending on the electron Fermi energy being on or off a quantum resonance of the scattering cavity. In comparison, for both 1D and 2D scattering problems involving a δ potential barrier, the sensitivity has been derived analytically in Ref. [13] and [10]. There, η_{11} shows strong spatial regular oscillations.

When the geometry parameter $H = W$, the conductor becomes a T-shaped junction. The upper panel of Fig. (4) shows η_{11} for this situation at $k_F W/\pi = 1.325$. The lower panel of Fig. (4) plots the characteristic potential $2u_1(\mathbf{r}) - 1$ for

this case. The quantity $2u_1(\mathbf{r}) - 1$ is interesting because it can easily be shown[8], using Eqs. (4), (5), (6) and applying the gauge invariance condition (11), that the nonlinear conductance can be re-written as

$$G_{\alpha\beta\gamma} = 4\pi\frac{e}{h} \int dE (-\partial_E f) \int d^3\mathbf{r} (\eta_{\alpha\beta} u_\gamma(\mathbf{r}) + \eta_{\alpha\gamma} u_\beta(\mathbf{r}) - \eta_{\alpha\beta} \delta_{\gamma\beta}) \quad . \quad (21)$$

Hence the quantity $2u_1(\mathbf{r}) - 1$ appears naturally in this form of G_{111} . From Fig. (4) it is clear that η_{11} is symmetric and $2u_1 - 1$ is anti-symmetric along x axis. As a result, G_{111} will be zero for this T-shaped junction if the scattering volume is symmetric due to the spatial integration of Eq. (21). To systematically investigate the behavior of G_{111} as the conductor shape changes from symmetric to asymmetric, we have calculated this quantity for several values of the geometric parameter H at zero temperature: $H = W, 1.25W, 1.5W$, and $1.75W$ (see Fig. (1)). Figs. (5a-5d) plot the DC-conductance G_{11} , the external and internal responses of the second order non-linear conductance, G_{111}^e [24], G_{111}^i , and G_{111} as a function of the normalized electron momentum $k_F W/\pi$ for these configurations. Several interesting features have been observed. First of all, the external (the internal) response of the second order non-linear conductance changes sign from negative (positive) to positive (negative) near the resonant point. This behavior is similar to that of one-dimensional asymmetric double barrier resonant tunneling[8]. In that case $G_{111} = (e^3/h)(dT/dE)(\Gamma_2 - \Gamma_1)/\Gamma$, where T is the transmission coefficient, Γ_i is the decay width of each barrier, and $\Gamma = \Gamma_1 + \Gamma_2$. Because of the term dT/dE , G_{111} changes sign across the resonant point and hence can be negative. The cancellation of the external and internal responses results in a much smaller G_{111} : one order of magnitude smaller than the internal or external contribution alone. Secondly, for $H = W$ the asymmetry of the scattering volume only comes from the location of the scattering volume boundary which is at our disposal, G_{111} has the smallest values for all $H < 2W$ studied. For $W < H < 2W$, the conductor is intrinsically asymmetric and G_{111} are larger. Also the resonance behavior of G_{111} becomes substantially sharper as H is increased. While G_{111} increases as H increases from $H = W$, it eventually starts to decrease after $H > 1.5W$. This is clearly seen from Fig. (5d) for which $H = 1.75W$. This is because for larger H the system approaches to the symmetric conductor at $H = 2W$, for which $G_{111} = 0$ as discussed above.

So far, as noted in Ref. [24], we have computed the external contribution G_{111}^e of Eq. (5) using a procedure which employs the gauge invariance condition. However if we directly use the right hand side of Eq. (5) to compute G_{111}^e , the result will not be accurate because the scattering volume is finite. In particular, as

studied previously[10] for a symmetric system G_{111} will be non-zero if calculated using the right hand side of Eq.(5). In terms of the gauge invariant condition, this will lead to a violation, *i.e.* $G_{111} + G_{112} \neq 0$. While such an error is not relevant if the scattering volume is very large, for our numerical calculations it will generate incorrect conclusions since the scattering volume is always finite. Hence, in order to use the right hand side to compute G_{111}^e , a correction term is needed to preserve the gauge invariance.

For a quasi-1D wire with a δ function impurity, this correction term has been derived[10] analytically. For that situation, the correction, C , consists of two terms[10]:

$$C = \frac{|s_{12}|^2}{k_1^2} Re(s_{11}) + Re\left(\sum_{n=2} \frac{b_1 |b_n|^2}{k_1 k_n} e^{ik_n(x_2 - x_1)}\right) . \quad (22)$$

where k_n is the longitudinal momentum for the n -th mode with $k_n^2 = k_F^2 - (n\pi/W)^2$ and $E = \hbar^2 k_F^2 / 2m$, x_1 and x_2 are the coordinates for the scattering boundaries, and b_n is the reflection scattering amplitude. Clearly, the first term is oscillating as the linear size of the scattering volume increases (due to s_{11}) and it is only relevant near the edge of the first propagation threshold; the second term is exponentially decaying to zero as the size of the volume increases and it comes solely from mode mixing and contributed by the evanescent modes. Although this form of the correction term was derived from another system, it is nevertheless interesting to compare this formula for the conductor studied here.

In Fig. (6) we plot the correction term Eq. (22) together with $G_{111} + G_{112}$ which were computed using the right hand side of Eq. (5), for the case $H = W$. Eq. (22) was evaluated using the scattering matrix elements obtained from our numerical calculation, and the system size ($x_2 - x_1$) was specified as the length of our scattering volume $2L + 2W$ (see Fig. (1)). For this conductor with $H = W$, we expect a good comparison with Eq. (22) which was derived for a δ -function scatterer inside a wire, because for both systems the geometric asymmetry is solely due to the positions of the scattering volume boundary. Other than that, these systems are actually *symmetric* with respect to the scattering potential. Indeed, Fig. (6) clearly shows that there is essentially no difference between Eq. (22) and our numerical data when the scattering volume is large ($L = 4W$). On the other hand, for a conductor with $H = 1.5W$ which has an intrinsically asymmetric scattering volume, the comparison is qualitative as shown in Fig. (7). However the trend of the two curves are still similar. We may thus conclude that for the gauge invariant condition, the correction term to the external contribution Eq. (5) has a form with the same nature as that of Eq. (22) above.

5 Summary

In this work we have developed a numerical technique based on a scattering matrix to compute the weakly nonlinear conductance. This technique is particularly useful for conductors whose scattering volume can be naturally divided into several regions. The most difficult step is the evaluation of the local electric current response, namely the sensitivity. We have reported how to obtain this quantity numerically, thus further investigations of the interesting nonlinear conductance problem can be carried out using our numerical method. We have found that sensitivity behaves differently when the transport energy is on or off resonance. The former leads to standing-wave type spatial dependence, while the latter is behaving in a less regular fashion. In all cases, the sensitivity shows spatial oscillating pattern, which is similar to those known from exact calculations for 1D models.

The nonlinear conductance can be non-zero only for geometrically asymmetric systems. The asymmetry can be introduced in two ways. The first is through the intrinsically asymmetrical shape of a conductor such as those of Fig. (1) with $W < H < 2W$. The other, which is a trivial asymmetry, is through the asymmetrical location of the scattering volume boundary, *e.g.* the case $H = W$. We discover that the intrinsic asymmetry leads to much larger nonlinear conductance than the other case. Furthermore, for the symmetrical scattering junction but with asymmetrical location of the boundary ($H = W$ case), for large size L the behavior of the gauge invariance condition agrees almost perfectly with Eq. (22) which was derived from a completely different system but also with the asymmetry introduced by the location of the scattering volume boundary only. On the other hand, such an agreement is less perfect for the intrinsically asymmetrical system. Hence we may conclude that the nonlinear conductance behaves in quite different manner depending on how the asymmetry is introduced.

The sign of the nonlinear conductance can be positive or negative. Very sharp variations of this quantity is discovered at quantum resonances for the conductor studied here, where such resonances are marked by sharp reductions of the linear conductance G_{11} . Hence near a resonance, the electric current may actually decrease for an increasing voltage difference by Eq. (3) since G_{111} is negative. Such a behavior is precisely the expected nonlinear conduction characteristic, and up to the second order in voltage difference our results can provide a prediction. Clearly, as the voltage difference becomes large, even higher order conductances must be included in order to have a meaningful prediction of the nonlinear I-V

curve.

Acknowledgments

We gratefully acknowledge support by a research grant from the Croucher Foundation, a RGC grant from the Government of Hong Kong under grant number HKU 261/95P, the NSERC of Canada and FCAR of Québec. We thank the Computer Center of the University of Hong Kong for computational facilities.

* permanent address: *Institute of Semiconductors,
Academia Sinica,
P. O. Box 912,
Beijing, P. R. China*

References

- [1] M. Büttiker, J. Phys. Condens. Matter **5**, 9361 (1993).
- [2] B. L. Al'tshuler and D. E. Khmelnitskii, JEPT Lett. **42**, 359 (1985).
- [3] N. S. Wingreen, A. P. Jauho, and Y. Meir, Phys. Rev. B **48**, 8487 (1993).
- [4] P. G. N. de Vegvar, Phys. Rev. Lett. **70**, 837 (1993).
- [5] R. Taboryski, A. K. Geim, M. Persson, and P. E. Lindelof, Phys. Rev. B **49**, 7813 (1994).
- [6] M. Büttiker, A. Prêtre, and H. Thomas, Phys. Rev. Lett. **70**, 4114 (1993).
- [7] M. Büttiker, H. Thomas and A. Prêtre, Z. Phys. B. **94**, 133 (1994).
- [8] T. Christen and M. Büttiker, Europhys. Lett. **35**, 523 (1996).
- [9] Jian Wang and Hong Guo, Phys. Rev. B **54**, R11090 (1996).
- [10] Jian Wang, Qingrong Zheng, and Hong Guo, to appear in Phys. Rev. B (April 15 1997-II).
- [11] Jian Wang, Qingrong Zheng, and Hong Guo, cond-mat/9703156.
- [12] We thank Prof. M. Büttiker for pointing this out to us (private communication).
- [13] V. Gasparian, T. Christen, and M. Büttiker, Phys. Rev. A. **54**, 4022 (1996).
- [14] M. Büttiker and T. Christen, in "Quantum Transport in Semiconductor Submicron Structures", edited by B. Kramer (Kluwer Academic Publishers, Dordrecht, 1996).
- [15] R. L. Schult, D. G. Ravenhall, and H. W. Wyld, Phys. Rev. B **39**, 5476 (1989).

- [16] P. A. Lee and D. S. Fisher Phys. Rev. Lett. **47**, 882 (1981).
- [17] H. U. Baranger, D. P. DiVincenzo, R. A. Jalabert, and A. D. Stone, Phys. Rev. B **44**, 10637 (1991).
- [18] M. J. McLennan, Y. Lee, and S. Datta, Phys. Rev. B **43**, 13846 (1991).
- [19] C. S. Lent and D. J. Kirkner, J. Appl. Phys. **67**, 6353 (1990).
- [20] Y. J. Wang, J. Wang, and H. Guo, Phys. Rev. B **49**, 1928 (1994); M. Leng and C. S. Lent, J. Appl. Phys. **76**, 2240 (1994).
- [21] W. D. Sheng, J. Phys. Condens. Matter (1997) (to be published).
- [22] H. Tamura and T. Ando, Phys. Rev. B **44**, 1792 (1991)
- [23] Y. Takagaki and D. K. Ferry, Phys. Rev. B **45**, 6716 (1992).
- [24] The G_{111}^e of Fig. (5) was computed by replacing the energy derivatives of Eq. (5) with a potential derivative using the gauge invariance condition. This procedure can be proven using the original formula in Ref. [14, 25] and numerically verified in Ref. [10].
- [25] C. R. Leavens and G. C. Aers, Solid State Commun. **67**, 1135 (1988); Phys. Rev. B **39**, 1202 (1989).

Figure Captions

- Fig. 1 Schematic view of an asymmetric cavity (the shaded area) embedded in a quantum wire.
- Fig. 2 The sensitivity η_{11} at three different positions, $(x, y) = \{(0.5W, 0.5W), (0.5W, 1.25W), (1.25, 0.625W)\}$, as a function of the normalized electron momentum $k_F W/\pi$ for $H = 1.25W$.
- Fig. 3 Three dimensional view of the sensitivity η_{11} for $H = 1.25W$ at two different values of the electron momentum $k_F W/\pi = 1.715$ and $k_F W/\pi = 1.795$.
- Fig. 4 Three dimensional view of the sensitivity η_{11} and the characteristic potential $2u_1 - 1$ for a symmetric T-shaped cavity at $k_F W/\pi = 1.325$ and $H = W$.
- Fig. 5 The DC-conductances G_{11} and the leading order nonlinear terms G_{111} as a function of the normalized electron momentum $k_F W/\pi$, solid lines for G_{111}^e and dotted lines for G_{111}^i . (a) $H = W$, (b) $H = 1.25W$, (c) $H = 1.5W$, (d) $H = 1.75W$. Here E_1 is the threshold of the first subband defined as $E_1 = \hbar^2 \pi^2 / (2mW^2)$.
- Fig. 6 $G_{111} + G_{112}$ (solid line) and the correction term according to Eq.(22) (dotted line) versus momentum for the T-shaped cavity ($H = W$). Upper panel: $L = 0$. Lower panel: $L = 4W$.
- Fig. 7 $G_{111} + G_{112}$ (solid line) and the correction term according to Eq.(22) (dotted line) versus momentum for an asymmetric structure ($H = 1.5W$). Upper panel: $L = 0$. Lower panel: $L = 4W$.

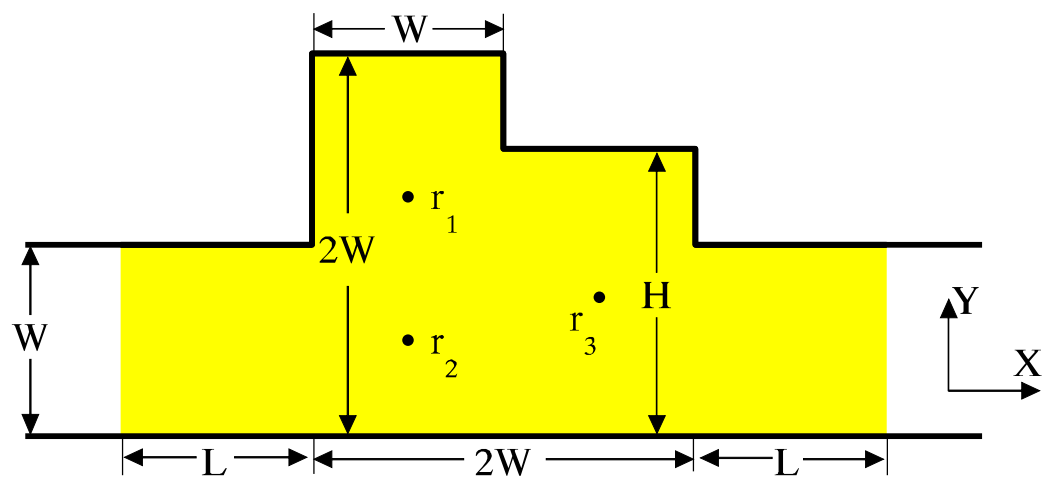


Fig. 1

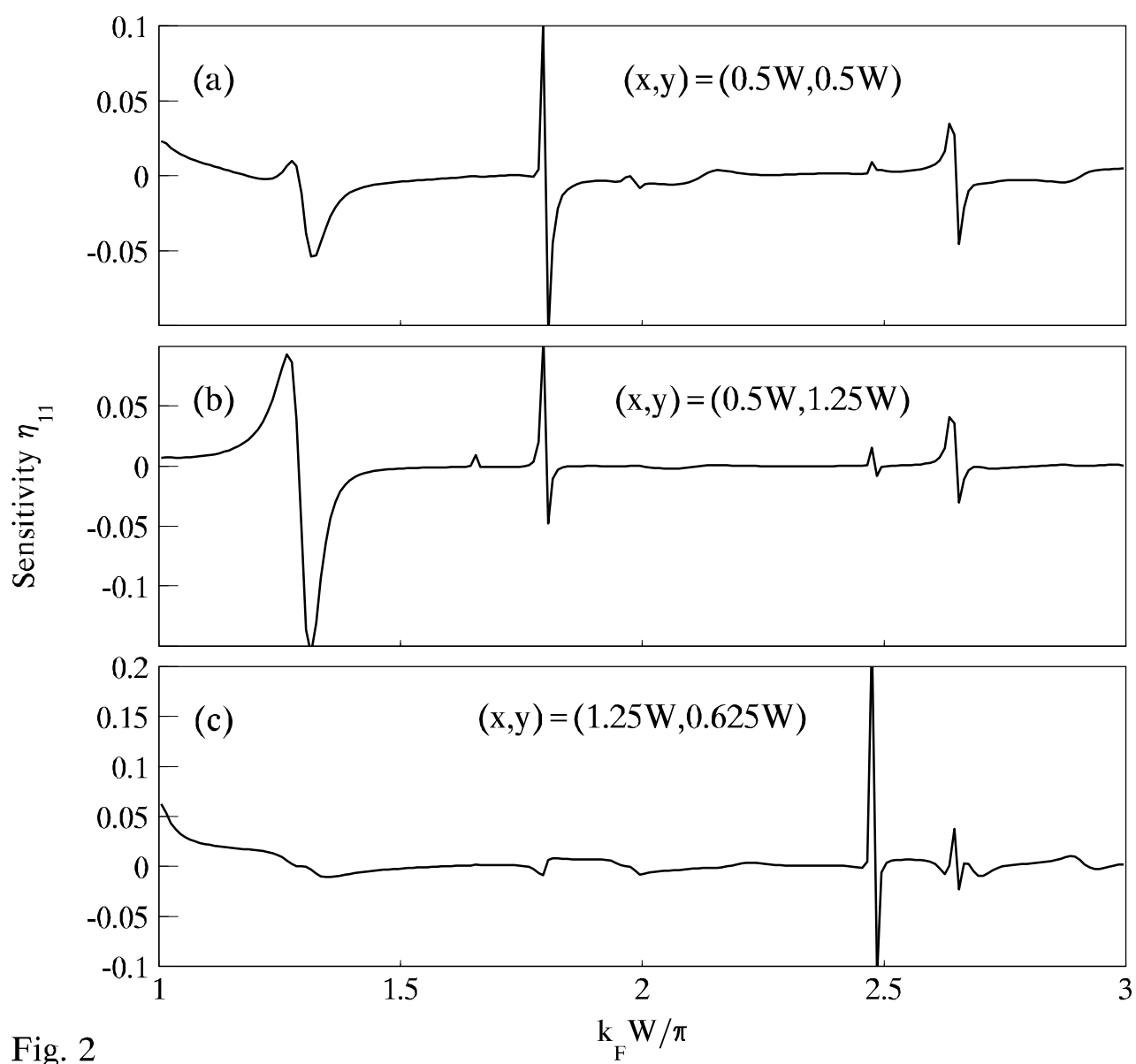


Fig. 2

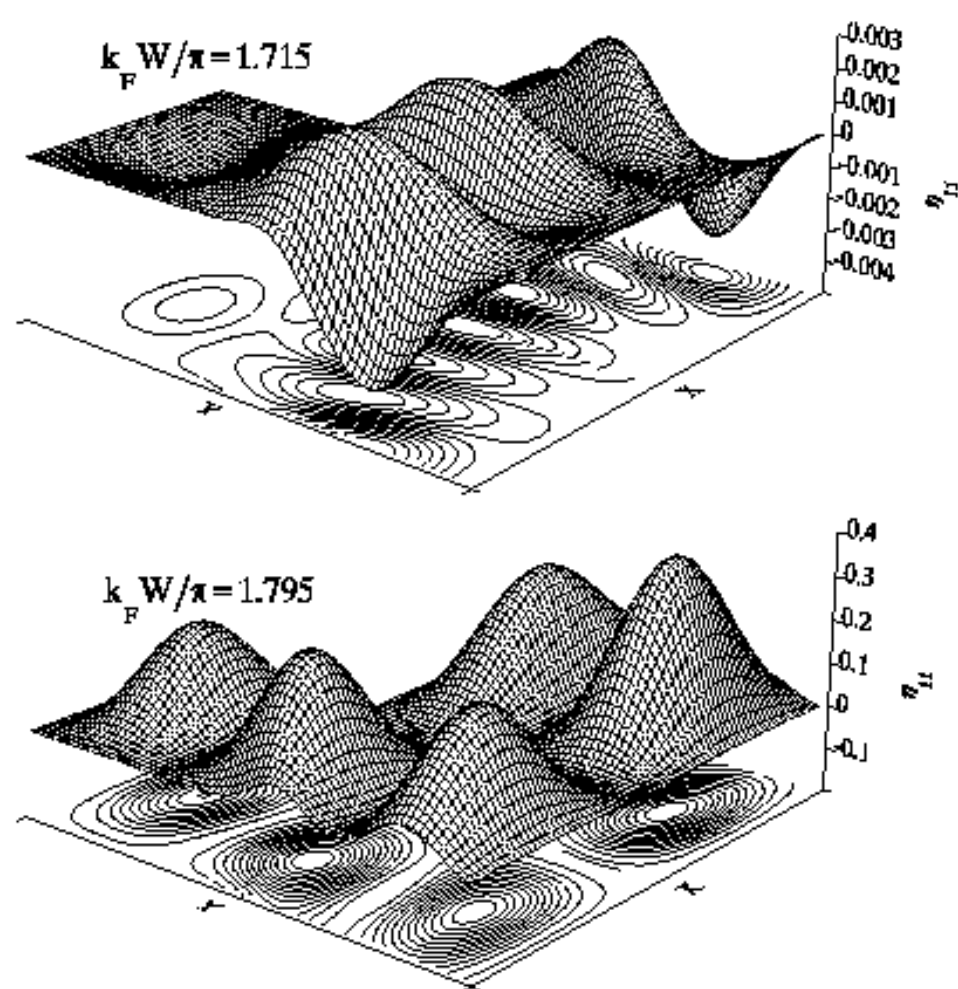


Fig. 3

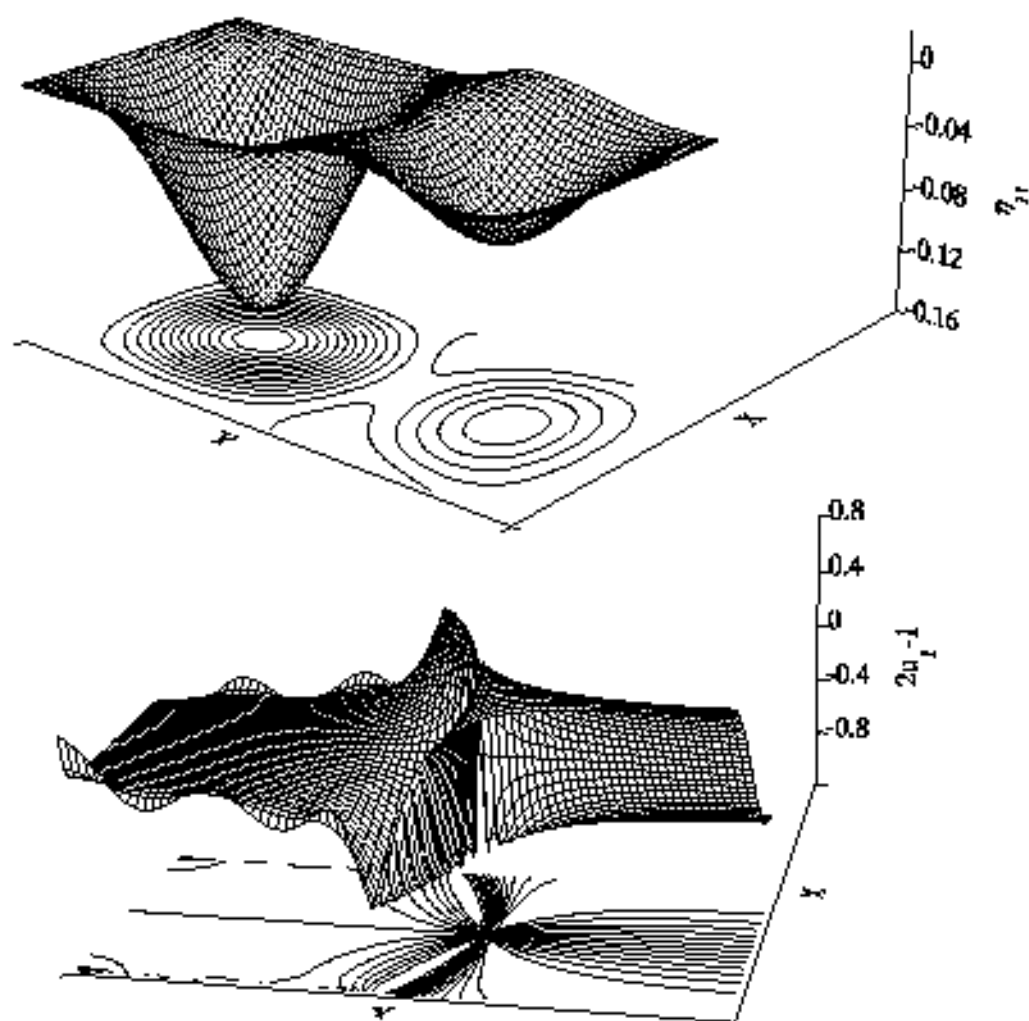


Fig. 4

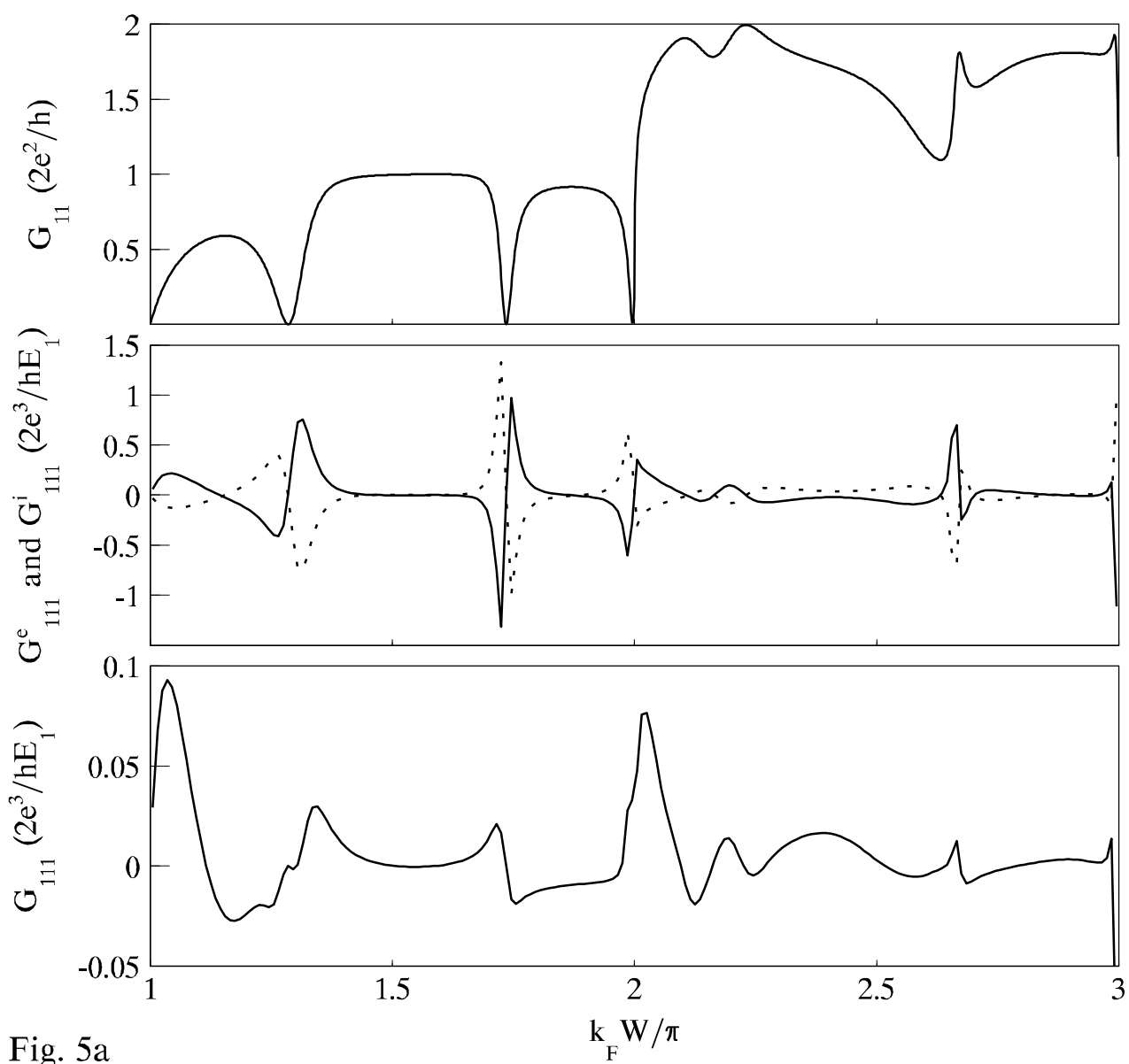


Fig. 5a

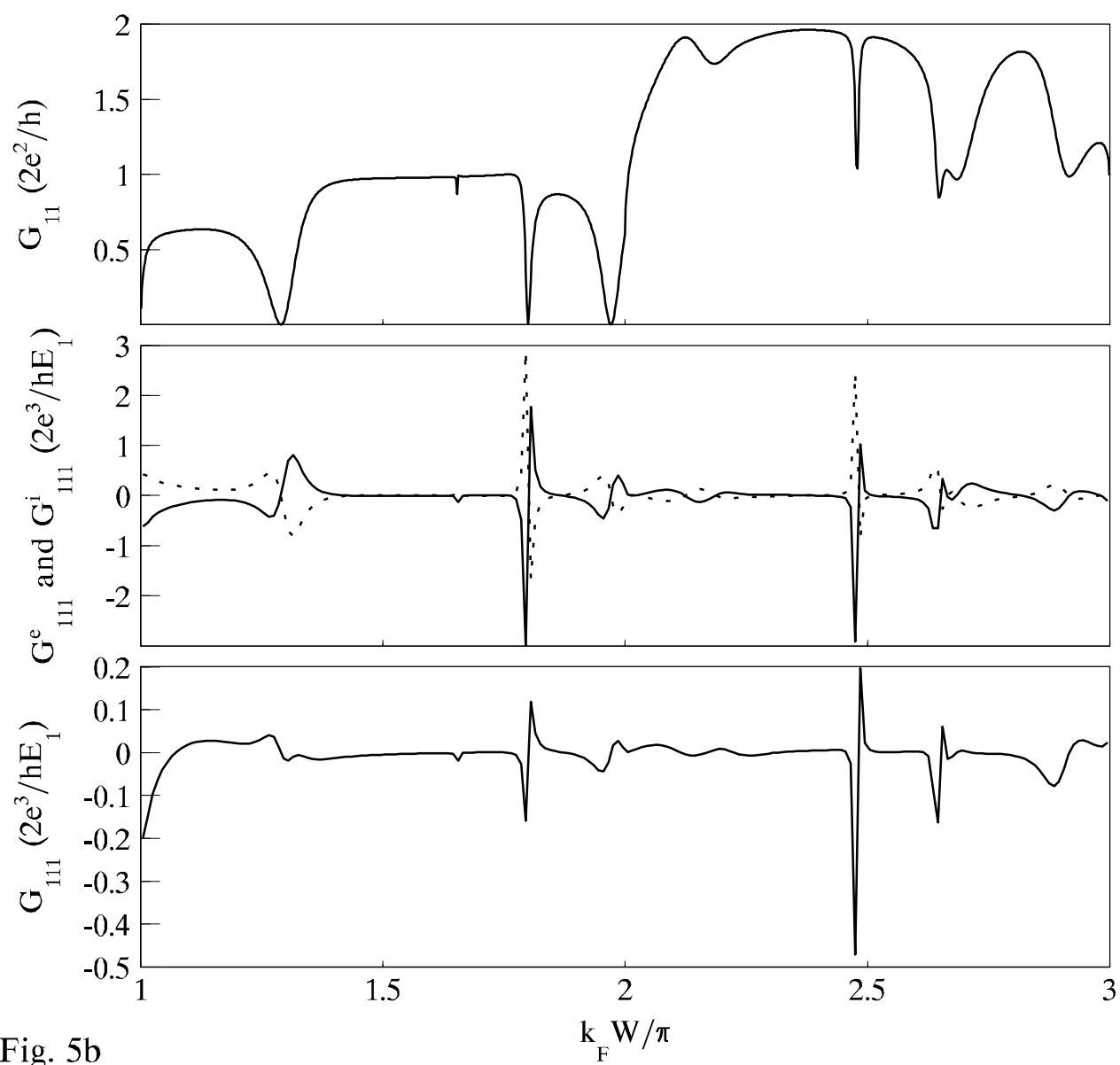


Fig. 5b

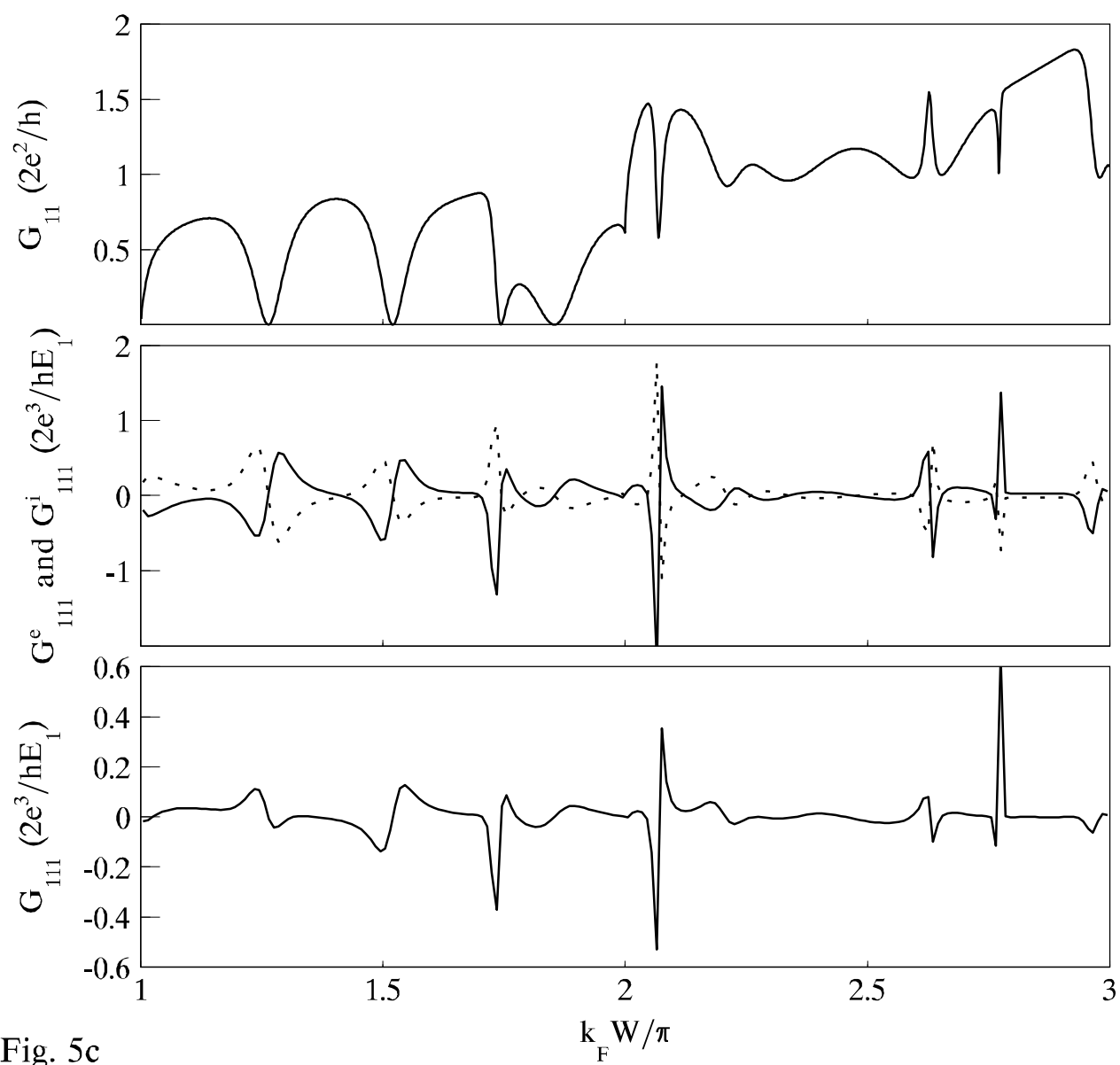


Fig. 5c

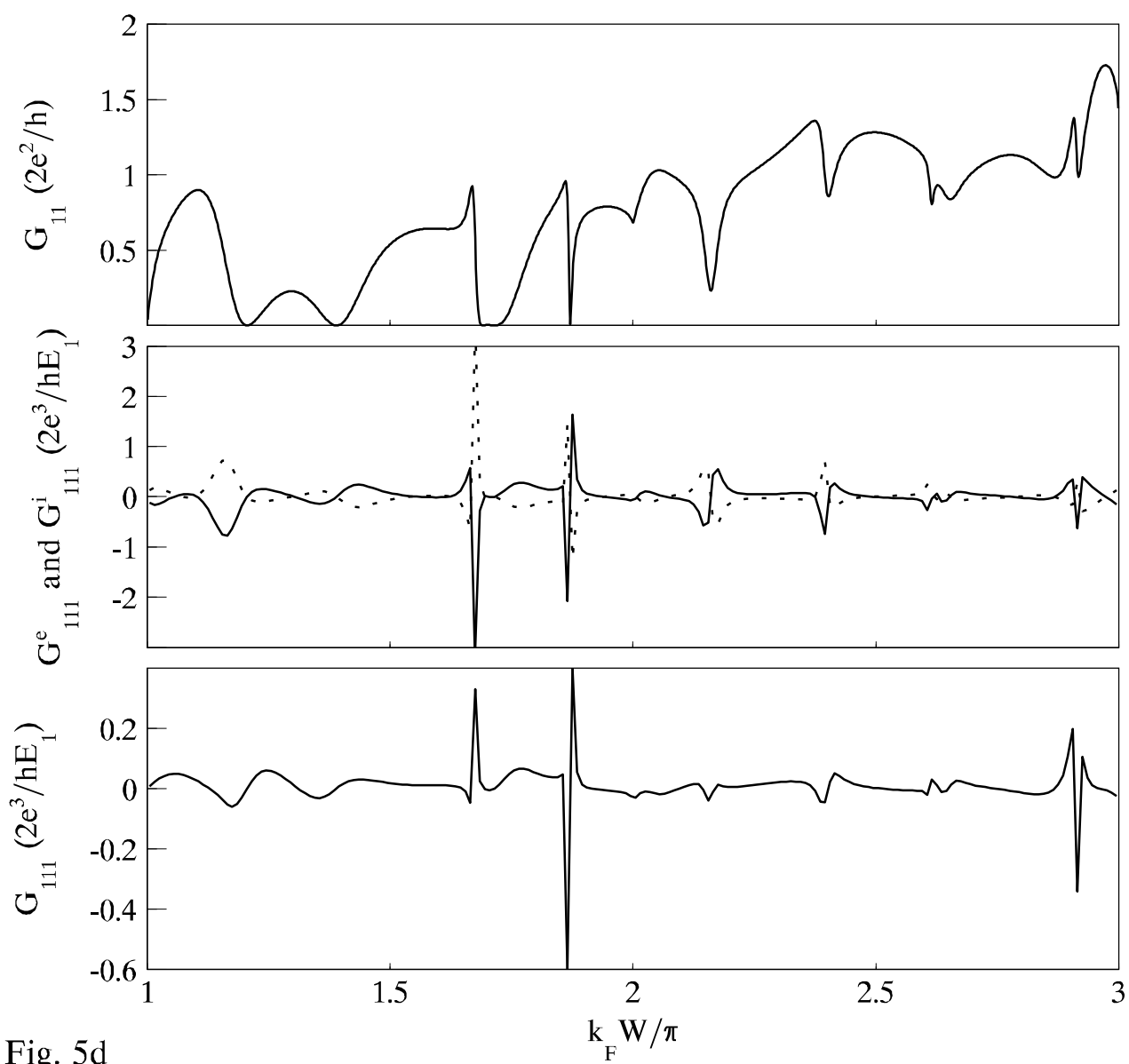


Fig. 5d

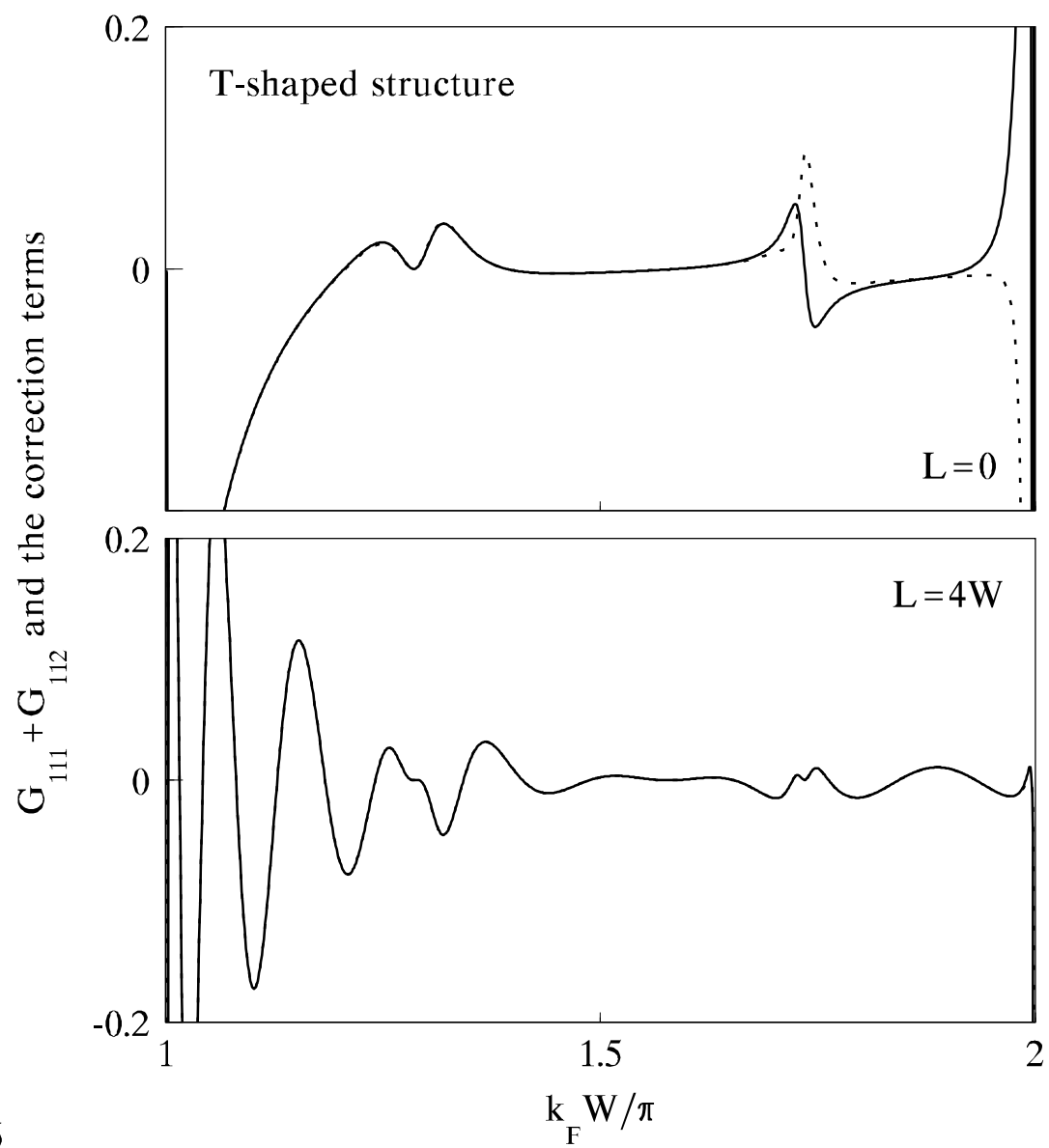


Fig. 6

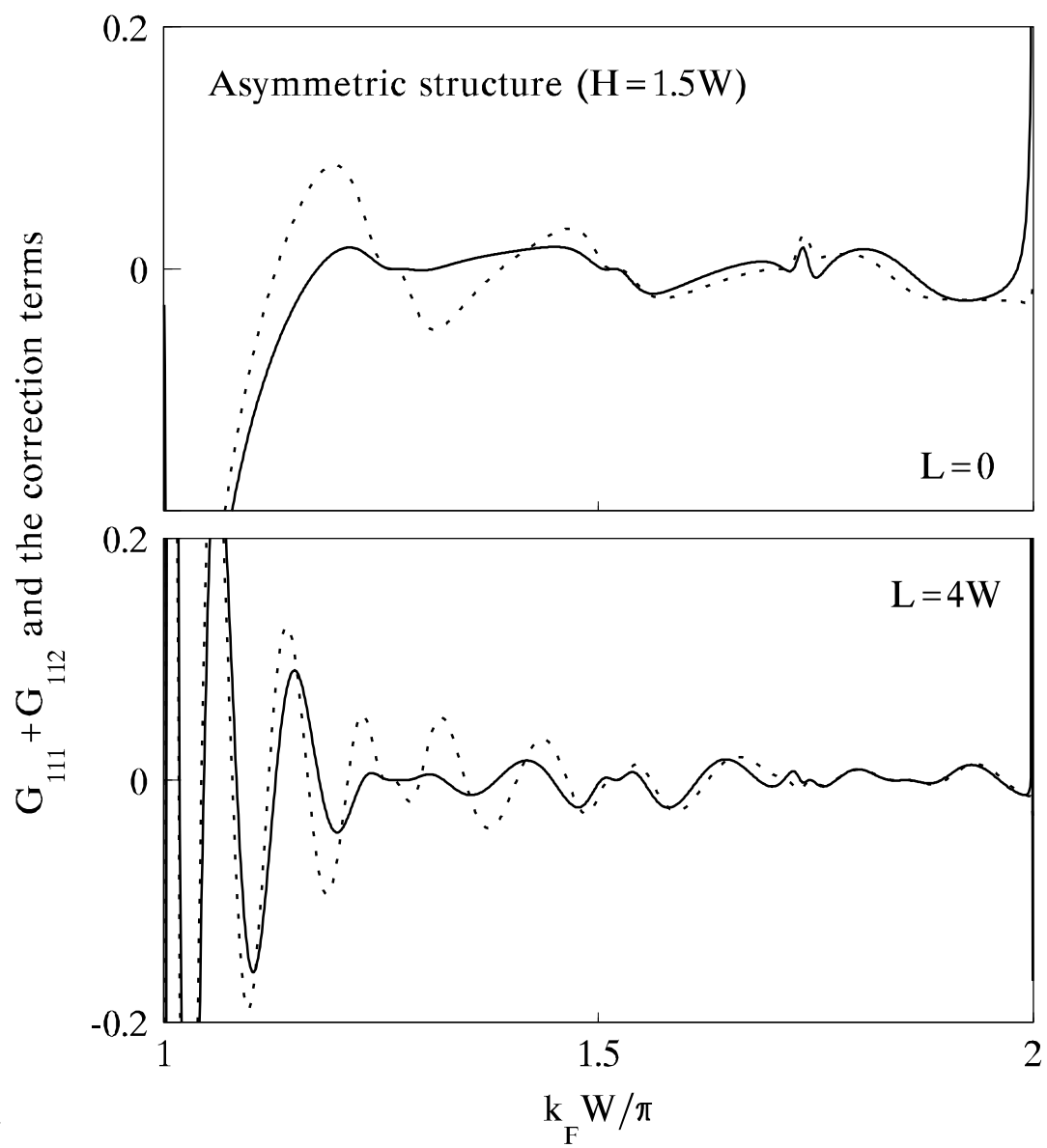


Fig. 7